



Syntheses and structures of metal–metal triply bonded M_2R_6 compounds: consideration of starting materials, stability, and structural parameters

Thomas M. Gilbert^{a,*}, Cary B. Bauer^c, Robin D. Rogers^{b,*}

^aDepartment of Chemistry and Biochemistry, Northern Illinois University, DeKalb, IL 60115, USA

^bDepartment of Chemistry, The University of Alabama, Tuscaloosa, AL 35487, USA

^cInstitute for Enzyme Research, University of Wisconsin, Madison, WI 53705, USA

Received 13 May 1998; accepted 6 November 1998

Abstract

The syntheses and structures of four homoleptic metal–metal triply-bonded M_2R_6 compounds [$Mo_2(CH_2CMe_2Ph)_6$, **1**; $Mo_2(CH_2SiMe_2Ph)_6$, **2**; $W_2(CH_2SiMe_2Ph)_6$, **3**; and $W_2(CH_2Ph)_6$, **4**] are reported. The synthetic effort suggests that ditungsten compounds are inherently more difficult to prepare and more thermally sensitive than dimolybdenum compounds, probably as a result of the larger dimetal core the ligands must protect. The structural data confirm that dimetal hexaalkyls exhibit shorter $M\equiv M$ distances than do dimetal hexaalkoxides, even in a matched pair case where steric differences are minimal. © 1999 Elsevier Science Ltd. All rights reserved.

Keywords: Metal–metal dimer; Triple bond; Alkyl; Homoleptic; X-ray structure; Distal ligand

1. Introduction

$Mo_2(CH_2SiMe_3)_6$ was the first M_2X_6 compound (M =a transition metal) to be synthesized, and the first shown crystallographically to contain an unsupported metal–metal triple bond [1]. Since then, numerous triply bonded M_2X_6 dimers containing pseudohalide ligands have appeared [2–4]. However, the number of homoleptic dimetal hexaalkyls has remained small; only $M_2(CH_2CMe_3)_6$ (M =Mo [5], W [6]), $W_2(CH_2SiMe_3)_6$ [7], and $Mo_2(CH_2Ph)_6$ [8] have been added to the list, and only the last two were characterized crystallographically.

One reason relatively few M_2R_6 compounds are known is that suitable preparation methods have proved difficult to find. $Mo_2(CH_2CMe_3)_6$, $M_2(CH_2SiMe_3)_6$ (M =Mo, W), and $Mo_2(CH_2Ph)_6$ were initially prepared from metal halides and alkyllithium or Grignard reagents in 2–20% yield. These reactions did not scale up well. More recently, Rothwell prepared $Mo_2(CH_2SiMe_3)_6$ (74% yield) [9] and $Mo_2(CH_2Ph)_6$ (29%) [8] from $Mo_2(O-i-Pr)_6$, Chisholm prepared $W_2(CH_2CMe_3)_6$ from $NaW_2Cl_7(THF)_5$ (55%) [6], and we prepared $Mo_2(CH_2CMe_3)_6$ and $Mo_2(CH_2SiMe_3)_6$ from “ $MoCl_3(dme)$ ” (73 and 84%,

respectively) [10], but the generality of these reactions has not been examined.

Our interest in this area arose from our Raman studies of the metal–metal stretching frequency in M_2X_6 dimers [11]. We needed a variety of M_2R_6 compounds, and felt this warranted investigating the utility of “ $MoCl_3(dme)$ ” and $NaW_2Cl_7(THF)_5$ in preparing them. We have found that “ $MoCl_3(dme)$ ” is a good starting material for other dimolybdenum hexaalkyls, but that preparing ditungsten hexaalkyls from $NaW_2Cl_7(THF)_5$ is problematic. Hexa-(alkoxy)ditungsten compounds are much better precursors for these. We report here four syntheses of dimetal hexaalkyls containing phenyl groups, and the crystal structures of the four compounds $Mo_2(CH_2CMe_2Ph)_6$, **1**; $Mo_2(CH_2SiMe_2Ph)_6$, **2**; $W_2(CH_2SiMe_2Ph)_6$, **3**; and $W_2(CH_2Ph)_6$, **4**. The structural data confirm that dimetal hexaalkyls exhibit the shortest metal–metal bond distances of any member of the M_2X_6 class, even when comparing compounds which are nearly isomorphous. Steric considerations appear to determine most of the core and peripheral structural parameters.

2. Experimental

Unless otherwise noted, all reactions and manipulations

*Corresponding authors.

were performed under an inert atmosphere employing standard Schlenk or glove box techniques. Solvents were evaporated in vacuo. Ether and hydrocarbon solvents were distilled from purple potassium diphenyl ketyl. Me_3SiCl was distilled from CaH_2 . “ $\text{MoCl}_3(\text{dme})$ ” [10] $\text{W}_2(\text{OCy})_6$ [12], $\text{W}_2(\text{OCMe}_3)_6$ [6], and LiCH_2Ph [13] were prepared by published methods. $\text{LiCH}_2\text{CMe}_2\text{Ph}$ and $\text{LiCH}_2\text{SiMe}_2\text{Ph}$ were prepared analogously to $\text{LiCH}_2\text{CMe}_3$ [14].

NMR spectra were obtained on a Bruker WA-200 spectrometer at ambient temperature; chemical shifts are reported as ppm downfield of tetramethylsilane.

2.1. Synthesis of $\text{Mo}_2(\text{CH}_2\text{CMe}_2\text{Ph})_6$, 1

Solid $\text{LiCH}_2\text{CMe}_2\text{Ph}$ (2.24 g, 16.0 mmol) was added in small portions from a powder addition funnel to a stirring slurry of “ $\text{MoCl}_3(\text{dme})$ ” (1.46 g, 5.00 mmol) in 1:1 ether/pentane (120 ml) at -40°C over 30 m. The mixture was then allowed to warm slowly to ambient temperature over 2 h, giving a dark red solution over a goopy grey precipitate. The solvent was evaporated, giving orange-brown solid. This was extracted with toluene until the extracts were colorless. The extracts were filtered through a 5 cm pad of silica gel in a frit, giving a dark red-brown solution and removing a sizable quantity of solid. The solvent was evaporated, and the residue dissolved in 4×20 ml portions of boiling heptane. The heptane extracts were filtered, combined, and cooled to -30°C . The precipitated product was filtered out, washed with cold pentane, and dried, giving yellow microflakes (0.270 g, 0.272 mmol, 11%). The sample for X-ray study was crystallized by slow cooling of a saturated heptane solution from near boiling to ambient temperature. $^1\text{H NMR}$ (C_6D_6): δ 7.24–7.10 (m, 5H, Ph H); 2.02 (s, 2H, CH_2); 1.36 (s, 6H, CH_3).

2.2. Synthesis of $\text{Mo}_2(\text{CH}_2\text{SiMe}_2\text{Ph})_6$, 2

A pentane solution (100 ml) of $\text{LiCH}_2\text{SiMe}_2\text{Ph}$ (2.50 g, 16.0 mmol) was added dropwise over 30 m to a stirring slurry of “ $\text{MoCl}_3(\text{dme})$ ” (1.46 g, 5.00 mmol) in 1:1 ether/pentane (60 ml) at -40°C . The mixture was then allowed to warm slowly to ambient temperature over 2 h, giving a dark red solution over a goopy grey precipitate. The solvent was evaporated, giving yellow-black solid. This was extracted with toluene until the extracts were colorless. The extracts were filtered through a 5 cm pad of silica gel in a frit, giving a clear, orange-yellow solution and removing a sizable quantity of solid. The solvent was evaporated, and the residue triturated with pentane. The bright yellow powder was filtered out, washed with cold pentane, and dried. A second crop was isolated by evaporating the mother liquor to 1/3 the original volume, and cooling it to -30°C . (Total yield: 0.970 g, 0.892 mmol, 36%). The sample for X-ray study was crystallized by slow cooling of a saturated heptane solution from near

boiling to ambient temperature. $^1\text{H NMR}$ (C_6D_6): δ 7.50–7.18 (m, 5H, Ph H); 1.76 (s, 2H, CH_2); 0.34 (s, 6H, CH_3).

2.3. Synthesis of $\text{W}_2(\text{CH}_2\text{SiMe}_2\text{Ph})_6$, 3

A stirring slurry of $\text{W}_2(\text{OCy})_6$ (0.962 g, 1.00 mmol) in pentane (100 ml) was cooled to -20°C and treated dropwise over 45 m with a pentane solution (100 ml) of $\text{LiCH}_2\text{SiMe}_2\text{Ph}$ (0.956 g, 6.12 mmol). The yellow cyclohexoxide slowly dissolved, giving a red, translucent solution. After the addition of alkyllithium was completed, the slurry was stirred for 1 h at -20°C , then allowed to warm slowly to ambient temperature over 1 h. After 36 h of stirring, the solution was filtered, and the solvent was evaporated, giving a mixture of orange and white solids. This was dissolved in ether, and the stirring solution was treated with 3 ml Me_3SiCl . Over the course of 1 h, white solid precipitated. The solution was filtered to remove the solid, and the volatiles were evaporated. The resulting red-orange semisolid was dissolved in pentane and cooled to -30°C . The orange powder which precipitated was filtered out, washed with cold pentane and dried (0.356 g, 0.282 mmol, 28%). The sample for X-ray study was crystallized from a saturated heptane solution at -30°C . $^1\text{H NMR}$ (C_6D_6): δ 7.49–7.17 (m, 5H, Ph H); 1.76 (s, 2H, CH_2); 0.35 (s, 6H, CH_3).

2.4. Synthesis of $\text{W}_2(\text{CH}_2\text{Ph})_6$, 4

A stirring solution of $\text{W}_2(\text{OCMe}_3)_6$ (1.61 g, 2.00 mmol) in ether (75 ml) was cooled to -10°C and treated dropwise over 30 m with an ethereal solution of LiCH_2Ph (70 ml of 0.180 M solution, 12.6 mmol). The solution reddened, then became a red slurry as red microcrystals precipitated. After the addition of alkyllithium was complete, the slurry was stirred for 30 m at -10°C , then allowed to warm slowly to ambient temperature over 1 h. The solvent was evaporated, giving orange-brown solid. This was triturated with heptane, filtered out, washed with pentane and dried, giving the product as a deep red powder (1.63 g, 1.78 mmol, 89%). It is crucial to avoid heating this material at any point, as it decomposes nearly completely after 1 h at 50°C . The crystal for X-ray study was grown from a saturated toluene solution at -30°C . $^1\text{H NMR}$ (C_6D_6): δ 7.08–6.54 (m, 5H, Ph H); 3.64 (s, 2H, CH_2).

2.5. Crystal structure determinations

Crystals were removed from the glovebox under a layer of heavy mineral oil for microscopic examination. Selected crystals were rapidly attached with silicone grease to a glass pin held in the goniometer head, and were both frozen in place and protected from the atmosphere by immediately cooling them in a stream of cold nitrogen gas.

Space groups were determined by inspection of reflection data and confirmed by the successful solution of the

Table 1
Crystal data and structure refinement

	1	2	3	4
Color and shape	Yellow plate	Yellow fragment	Orange fragment	Red fragment
Crystal size, mm	0.30×0.20×0.10	0.12×0.10×0.10	0.09×0.20×0.23	0.10×0.20×0.30
Formula	C ₆₀ H ₇₈ Mo ₂	C ₅₄ H ₇₈ Mo ₂ Si ₆	C ₅₄ H ₇₈ W ₂ Si ₆	C ₄₂ H ₄₂ W ₂
Temperature, K	293 (2)	173 (2)	293 (2)	173 (2)
Crystal system/space group	Triclinic/ <i>P</i> $\bar{1}$	Monoclinic/ <i>P</i> 2 ₁ / <i>n</i>	Monoclinic/ <i>P</i> 2 ₁ / <i>n</i>	Rhombohedral/ <i>R</i> $\bar{3}$
Reflections used for unit cell (over full θ range)	430	8201	5432	1768
Unit cell dimensions: (Å, deg)	<i>a</i> 12.4296 (14) <i>b</i> 12.562 (2) <i>c</i> 18.856 (2) α 91.648 (5) β 92.152 (5) γ 115.600 (4)	12.890 (10) 18.003 (7) 13.394 (8) 90 111.51 (3) 90	11.4155 (6) 13.7875 (7) 18.6577 (9) 90 92.16 (1) 90	14.7534 (6) 14.7534 (6) 13.3371 (10) 90 90 120
<i>Z</i>	2	2	2	3
θ range, deg	1.82–23.25	1.88–23.29	1.84–23.47	2.21–23.29
Index ranges	–13 ≤ <i>h</i> ≤ 7 –12 ≤ <i>k</i> ≤ 13 –18 ≤ <i>l</i> ≤ 20	–12 ≤ <i>h</i> ≤ 14 –9 ≤ <i>k</i> ≤ 18 –14 ≤ <i>l</i> ≤ 7	–10 ≤ <i>h</i> ≤ 12 –15 ≤ <i>k</i> ≤ 14 –20 ≤ <i>l</i> ≤ 19	–4 ≤ <i>h</i> ≤ 16 –13 ≤ <i>k</i> ≤ 13 –13 ≤ <i>l</i> ≤ 14
Reflections collected	7933	5309	10032	2058
Independent reflections	6266 (<i>R</i> _{int} = 0.0328)	3791 (<i>R</i> _{int} = 0.0537)	4152 (<i>R</i> _{int} = 0.2052)	805 (<i>R</i> _{int} = 0.0305)
Observed reflections ^a	6259	3443	4145	764
Absorption coefficient, mm ^{–1}	0.509	0.590	4.071	6.886
Range of relat. transm. factors	0.94–0.65	0.9962–0.7683	0.9745–0.5430	0.9183–0.5963
Data/restraints/parameters	6259/0/572	3788/0/281	4145/0/287	803/0/67
Extinction coefficient	0.0030 (4)	0.014 (2)	0.0006 (2)	
SHELX-93 weight parameters ^b	0.0649, 4.2361	0.1301, 3.2094	0.0593, 2.2655	0.0085, 34.6981
<i>R</i> indices [<i>I</i> > 2σ(<i>I</i>)] ^c	<i>R</i> 1 = 0.0388, <i>wR</i> 2 = 0.1020	<i>R</i> 1 = 0.0660, <i>wR</i> 2 = 0.1699	<i>R</i> 1 = 0.0508, <i>wR</i> 2 = 0.1057	<i>R</i> 1 = 0.0260, <i>wR</i> 2 = 0.0574
<i>R</i> indices (all data)	<i>R</i> 1 = 0.0484, <i>wR</i> 2 = 0.1224	<i>R</i> 1 = 0.0702, <i>wR</i> 2 = 0.1781	<i>R</i> 1 = 0.0790, <i>wR</i> 2 = 0.1291	<i>R</i> 1 = 0.0282, <i>wR</i> 2 = 0.0594
GOF ^d	0.951	1.038	1.043	1.128

^a Corrected for Lorentz/polarization effects and empirically corrected for absorption (ψ -scans); $I_o > 2\sigma(I_o)$.

^b SHELXTL weight $w = [\sigma^2(F_o)^2 + (a*P)^2 + b*P]^{-1}$, where $P = (\text{Max}(F_o^2, 0) + 2F_c^2)/3$, and a and b are the values given.

^c $R = \sum ||F_o| - |F_c|| / \sum |F_o|$; $wR2 = \{\sum w(F_o^2 - F_c^2)^2 / \sum w(F_o^2)^2\}^{1/2}$.

^d $\text{GOF} = [\sum w(F_o^2 - F_c^2)^2 / (N_o - N_v)]^{1/2}$; N_o = number of observations, N_v = number of variables.

structures. Data for 1–4 were collected on a Siemens SMART diffractometer employing a CCD area detector, using graphite monochromated Mo K α radiation ($\lambda = 0.71073$ Å). Data collection and refinement parameters

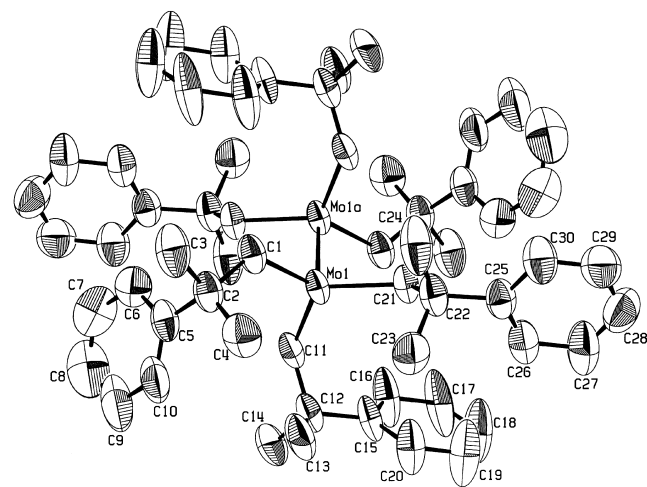


Fig. 1. ORTEP-III diagram of one of the independent molecules of Mo₂(CH₂CMe₂Ph)₆, **1**. Hydrogen atoms were removed for clarity.

appear in Table 1. Solutions and refinements were carried out using SHELXTL, refining on F^2 values [15]. All nonhydrogen atoms were refined with anisotropic temperature factors. Phenyl hydrogen atoms were placed in calculated positions and allowed to ride on the bonded carbon atom, with $U(\text{H}) = 1.2*U_{\text{eqv}}(\text{C})$. Methyl hydrogen atoms were included as a rigid group with rotational freedom at the bonded carbon atom, with $U(\text{H}) = 1.2*U_{\text{eqv}}(\text{C})$. ORTEP-III [16] diagrams of 1–4 appear in Figs. 1–4, respectively; selected distance and angle values appear in Table 2.

3. Results and discussion

3.1. Mo₂(CH₂CMe₂Ph)₆, **1**

Treatment of “MoCl₃(dme)” with three equivalents of LiCH₂CMe₂Ph provides yellow **1** in poor yield. The low yield is surprising given that the identical reaction between the trichloride and either LiCH₂CMe₃ or LiCH₂SiMe₃ gives the hexa(neopentyl)- or hexa(trimethylsilylmethyl)-dimolybdenum compounds in >70% yield [10]. Once

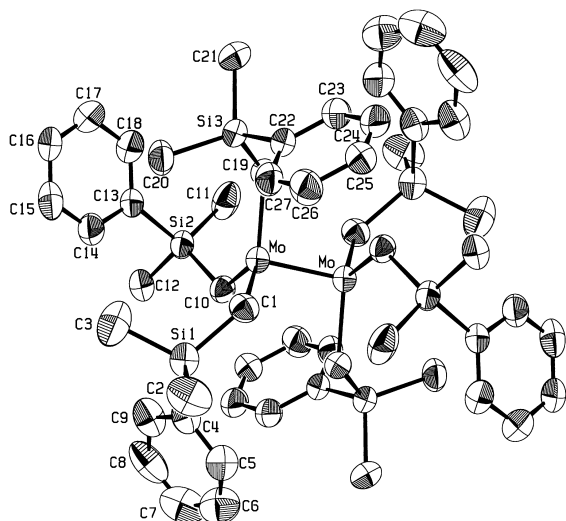


Fig. 2. ORTEP-III diagram of $\text{Mo}_2(\text{CH}_2\text{SiMe}_2\text{Ph})_6$, **2**. Hydrogen atoms were removed for clarity.

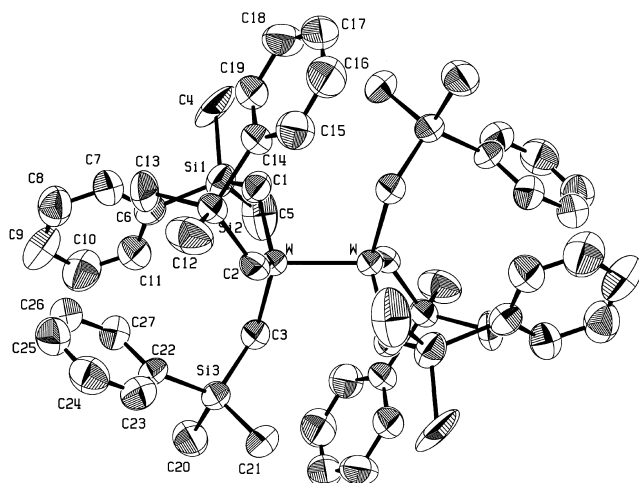


Fig. 3. ORTEP-III diagram of $\text{W}_2(\text{CH}_2\text{SiMe}_2\text{Ph})_6$, **3**. Hydrogen atoms were removed for clarity.

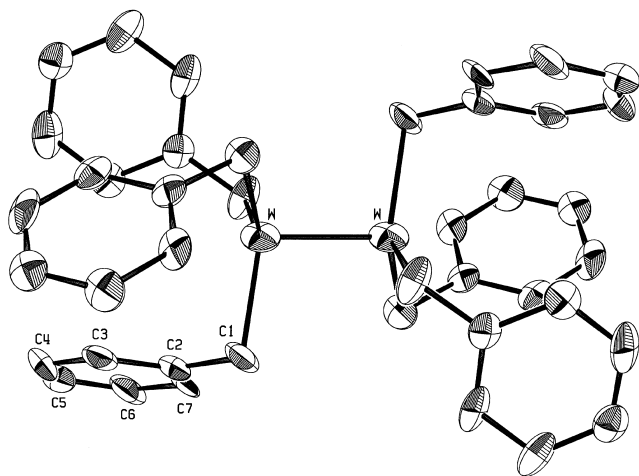


Fig. 4. ORTEP-III diagram of $\text{W}_2(\text{CH}_2\text{Ph})_6$, **4**. Hydrogen atoms were removed for clarity.

isolated, **1** shows thermal and air stability similar to those of the trimethylalkyl dimers.

In common with $\text{Mo}_2(\text{CH}_2\text{SiMe}_3)_6$ [1], **1** crystallizes with more than one dimer in the asymmetric unit. The two independent molecules exhibit identical structural parameters within experimental error (Table 2). The distances and angles associated with the M_2C_6 core are entirely consistent with those reported for the hexa(trimethylsilylmethyl) dimer and $\text{Mo}_2(\text{CH}_2\text{Ph})_6$ [8], with slight differences attributable to steric issues. For example, the average M–C distances in $\text{Mo}_2(\text{CH}_2\text{SiMe}_3)_6$ [2.131 (?) Å], **1** [2.135 (5, 9, 6) Å] [17], and **2** [2.113 (5, 11, 3) Å] are experimentally identical, and shorter than that in $\text{Mo}_2(\text{CH}_2\text{Ph})_6$ [2.162 (2) Å] [18]. We think the difference arises from the need for the six ligands to “protect” the dimetal core; in $\text{Mo}_2(\text{CH}_2\text{Ph})_6$, containing the smallest ligand, the metal–carbon distance lengthens to better allow the benzyl group to do this. Evidence for this theory appears in the angle data: while the Mo–Mo–C angles of all four dimolybdenum hexaalkyls are similar [97.89 (14, 34, 6)° for **1**; 99.7 (2, 12, 3)° for **2**; 100.6 (?)° for $\text{Mo}_2(\text{CH}_2\text{SiMe}_3)_6$; 97.61 (6)° for $\text{Mo}_2(\text{CH}_2\text{Ph})_6$], the Mo–C–C(Si) angles track the relative sizes of the groups attached to the methylene carbon [125.0 (3, 9, 6)° for **1**; 122.0 (3, 16, 3)° for **2**; 121.1 (?)° for $\text{Mo}_2(\text{CH}_2\text{SiMe}_3)_6$; 98.9 (1)° for $\text{Mo}_2(\text{CH}_2\text{Ph})_6$]. The much more acute angle in the hexabenzyl compounds denotes phenyl rings which are tipped back toward the dimetal core as a protective mechanism. It should be noted that this tipping is entirely steric in origin; no short contacts between the molybdenum and the 2- and 6-carbons of the phenyl ring were observed in $\text{Mo}_2(\text{CH}_2\text{Ph})_6$, and thus no η^3 benzyl–metal interactions exist.

In our study of $\text{M}_2(\text{OR})_6$ compounds containing tertiary alkoxides [19] we noted consistent differences between the bond and angle values for proximal alkoxides (those where the alkoxide group lies over the metal–metal triple bond, and for which the M–M–O–C torsion angle is near 0°) and those for distal alkoxides (those where the alkoxide group points away from the metal–metal triple bond, and for which the M–M–O–C torsion angle is near 180°). It would have been valuable to determine whether this holds for dimetal hexaalkyls, but intriguingly, every such dimer characterized by diffraction methods, including **1–4**, crystallizes in a nearly “all distal” motif. The Mo–Mo–CH₂–C torsion angles in **1** average 144.5 (8, 3.4, 6)°. This value is lowered from the ideal 180° (probably by the steric crowding that would arise from three perfectly distal ligands on one metal), but is far larger than the expected 0° for a proximal ligand. This provides a distinct contrast to $\text{M}_2(\text{OR})_6$ compounds, where only one all-distal conformation has been observed.

Compound **1** and $\text{Mo}_2(\text{OCMe}_2\text{Ph})_6$ [19] are “peripherally identical”: they contain ligands identical save for the bonded atom. They thus provide a matched pair for comparison of the effect of the bonded atom on the dimetal

Table 2
Selected bond distances (Å) and angles (°) for **1–4**

Atoms	1 (M=Mo)	2 (M=Mo)	3 (M=W)	4 (M=W)
M≡M	2.1765 (8) (Mo1–Mo1a) 2.1768 (7) (Mo2–Mo2a)	2.170 (2) (Mo–Mo')	2.2587 (5) (W–W')	2.2492 (9) (W–W')
M–C	2.138 (5) (Mo1–C1) 2.125 (5) (Mo1–C11) 2.138 (5) (Mo1–C21) 2.134 (4) (Mo2–C31) 2.125 (4) (Mo2–C41) 2.147 (5) (Mo2–C51)	2.126 (6) (Mo–C1) 2.108 (5) (Mo–C11) 2.106 (5) (Mo–C21)	2.101 (7) (W–C1) 2.116 (7) (W–C2) 2.105 (7) (W–C3)	2.156 (6) (W–C1)
C–C/Si	1.545 (7) (C1–C2) 1.550 (7) (C11–C12) 1.551 (6) (C21–C22) 1.554 (6) (C31–C32) 1.555 (6) (C41–C42) 1.560 (7) (C51–C52)	1.868 (5) (C1–Si1) 1.875 (5) (C10–Si2) 1.876 (6) (C19–Si3)	1.856 (7) (C1–Si1) 1.845 (6) (C2–Si2) 1.860 (7) (C3–Si3)	1.492 (7) (C1–C2)
M–M–C	97.83 (14) (Mo1–Mo1a–C1) 97.64 (14) (Mo1–Mo1a–C11) 97.82 (14) (Mo1–Mo1a–C21) 98.21 (13) (Mo2–Mo2a–C31) 97.47 (13) (Mo2–Mo2a–C41) 98.38 (13) (Mo2–Mo2a–C51)	98.9 (2) (Mo–Mo'–C1) 101.1 (2) (Mo–Mo'–C10) 99.0 (2) (Mo–Mo'–C19)	101.9 (2) (W–W'–C1) 102.2 (2) (W–W'–C2) 102.2 (2) (W–W'–C3)	98.36 (14) (W–W'–C1)
C–M–C	116.2 (2) (C1–Mo1–C11) 120.9 (2) (C1–Mo1–C21) 117.5 (2) (C11–Mo1–C21) 118.8 (2) (C31–Mo2–C41) 116.6 (2) (C31–Mo2–C51) 118.9 (2) (C41–Mo2–C51)	117.4 (2) (C1–Mo–C10) 118.4 (2) (C1–Mo–C19) 115.9 (2) (C10–Mo–C19)	115.9 (3) (C1–W–C2) 114.9 (3) (C1–W–C3) 116.4 (3) (C2–W–C3)	117.92 (7) (C1–W–C1')
M–C–C/Si	124.9 (4) (Mo1–C1–C2) 125.1 (3) (Mo1–C11–C12) 126.8 (3) (Mo1–C21–C22) 124.2 (3) (Mo2–C31–C32) 124.6 (4) (Mo2–C41–C42) 124.3 (3) (Mo2–C51–C52)	123.8 (3) (Mo–C1–Si1) 121.7 (3) (Mo–C10–Si2) 120.6 (3) (Mo–C19–Si3)	125.8 (4) (W–C1–Si1) 122.7 (3) (W–C2–Si2) 122.0 (4) (W–C3–Si3)	100.1 (3) (W–C1–C2)

core, although one must remember that the two are not isomorphous. In the discussion below, we include only parameters for the distal alkoxide ligands of $\text{Mo}_2(\text{OCMe}_2\text{Ph})_6$ so as to compare only ligands of like conformation.

The notable feature of the pair is that the core angles match well. The Mo–Mo–O angles in $\text{Mo}_2(\text{OCMe}_2\text{Ph})_6$ average 97.10 (7, 20, 2)°, while the Mo–Mo–C angles in **1** average 97.89 (14, 34, 6)°. The Mo–O–C angles in $\text{Mo}_2(\text{OCMe}_2\text{Ph})_6$ average 128.2 (2, 4, 2)°, while the Mo–CH₂–C angles in **1** average 125.0 (3, 10, 6)°. That the methylene group in **1** is larger than the oxygen in the hexaalkoxide has little impact on the internal conformation of the molecules.

The one feature of the M_2X_6 cores which clearly distinguishes the hexaalkoxide dimer from the hexaalkyl dimer is the metal–metal bond length. In $\text{Mo}_2(\text{OCMe}_2\text{Ph})_6$, the Mo≡Mo distance is 2.2388 (6) Å, while in **1** the distances average 2.1767 (8, 2, 2) Å, 0.06 Å shorter. It was recognized in the mid-1970s that the Mo≡Mo bond length of $\text{Mo}_2(\text{CH}_2\text{SiMe}_3)_6$ (2.167 Å) appeared shorter than that in $\text{Mo}_2(\text{NMe}_2)_6$ [2.214 (3) Å] [20] and in $\text{Mo}_2(\text{OCH}_2\text{CMe}_3)_6$ [2.222 (2) Å] [21] but the paucity of data and the structural diversity of the molecules limited

the conclusions that could be drawn. For example, one could argue that the Mo≡Mo bond in $\text{Mo}_2(\text{NMe}_2)_6$ lengthens to lessen steric contacts between dimethylamino methyl groups on opposite metals, while this is unnecessary in $\text{Mo}_2(\text{CH}_2\text{SiMe}_3)_6$, where rotation about the methylene group can decrease repulsions. The matched pair here, however, provides clear evidence that hexaalkyls exhibit *inherently* shorter metal–metal bond distances than do hexaalkoxides.

To what should the phenomenon be attributed? Since steric effects/ligand conformations appear irrelevant, there are only two obvious candidates. One is the presence of O $\pi \rightarrow \text{M} \pi^*$ donation in the hexaalkoxides lengthening the M≡M bond; the other is the greater electronegativity of oxygen vs. carbon forcing a larger effective positive charge on the metals in the hexaalkoxides, in turn causing them to repel each other and decrease metal orbital overlap [3]. The two represent limiting cases of the relationship between electron density and bond length: in the former, the metal–metal bond length increases because ligand atoms add electron density to the metals, while in the latter, the metal–metal bond length increases because ligand atoms withdraw electron density from the metals. As we discuss in the accompanying paper [19], collected

structural evidence suggests that M–O π interaction contributes little to the bonding picture in $M_2(OR)_6$ species. Furthermore, postulating an effective charge increase in $M_2(OR)_6$ compounds is crucial in explaining photoelectron spectroscopic experiments to be reported elsewhere [22]. So it appears the metal–metal bond is shorter in **1** because the $M(CH_2CMe_2Ph)_3$ moieties do not repel each other as much as the $M(OCMe_2Ph)_3$ fragments in $Mo_2(OCMe_2Ph)_6$ do.

3.2. $Mo_2(CH_2SiMe_2Ph)_6$, **2**, and $W_2(CH_2SiMe_2Ph)_6$, **3**

Treating “ $MoCl_3(dme)$ ” with $LiCH_2SiMe_2Ph$ gives dimer **2** in acceptable yield [though still quite a bit smaller than that of $Mo_2(CH_2SiMe_3)_6$] after minimal workup. Preparing the ditungsten homologue **3** is considerably more difficult. We attempted several times to prepare it from $NaW_2Cl_7(THF)_5$, the most generally useful tungsten (III) halide starting material, but were unable to isolate more than a few crystals of the hexaalkyl dimer. Using $W_2(OCMe_3)_6$ proved no more successful. Ultimately we found that treating $W_2(OCy)_6$ with the alkyllithium followed by Me_3SiCl to remove the $LiOCy$ byproduct led to **3** in acceptable yield, on a useful scale.

The original report of the structure of $Mo_2(CH_2SiMe_3)_6$ stated that the ditungsten analogue $W_2(CH_2SiMe_3)_6$ exhibited nearly identical cell parameters and the identical space group and thus was isostructural [1]. However, the full details have never been published, and Chisholm and coworkers later found that they were unable to refine data from a crystal with these cell parameters. They solved the structure using a crystal in which the tungsten dimer crystallized in a different space group, with different cell parameters [7]. Compounds **2** and **3** provide a complement to this curiosity: they crystallize in cells with quite different parameters, but in the same space group.

The two homologues are nearly isostructural save that the $Mo\equiv Mo$ bond length is shorter than the $W\equiv W$ bond length by the usual 0.07 Å. It appears the M–M–C angle in **2** is slightly more acute [99.7 (2, 12, 3)°] than that in **3** [102.1 (2, 2, 3)°], but the data are insufficient to demonstrate this unambiguously. Furthermore, the corresponding values for $Mo_2(CH_2SiMe_3)_6$ [100.6 (?)°] and $W_2(CH_2SiMe_3)_6$ [101.7 (10, 21, 12)°] are experimentally identical. Providing some corroboration for the difference, however, are the M–M–C–Si torsion angles, which average to 126.2 (7, 2.7, 3)° for **2** and 118.3 (9, 1.6, 3)° for **3**. As one would expect, the smaller torsion angle correlates with the larger M–M–C angle which determines it. Nonetheless, it does not seem that the larger $W\equiv W$ core in **3** has a dramatic impact on the conformations of the ligands. Combined with our comments above regarding $Mo_2(CH_2Ph)_6$, it appears ligand size dictates ligand conformation more than does the size of the core the ligand must protect.

Despite the presence of the larger, more polarizable

silicon atom in **2**, the structures of **1** and **2** are strikingly similar. In particular, the M–C–C angles in **1** are experimentally identical to the M–C–Si angles in **2**, indicating that the larger silicon atom is too far removed from the dimetal core to affect it. The size difference manifests itself solely in the M–M–C–C(Si) torsion angles, which are 144.5 (8, 3.4, 6)° for **1** and 126.2 (7, 2.7, 3)° for **2**. This is straightforward to rationalize based on steric considerations: the ligand with the larger silicon atom (and therefore longer CH_2-X and $X-CH_3$ distances) can more readily bend back toward the dimetal core and lower the torsion angle.

Comparisons between **2** and $Mo_2(CH_2SiMe_3)_6$ and **3** and $W_2(CH_2SiMe_3)_6$ demonstrate that the added steric bulk of the phenyl groups in the dimethylphenylsilylmethyl systems causes little if any molecular distortion in the M_2C_6 core. The core distances and angles in each pair of compounds are identical within experimental error.

3.3. $W_2(CH_2Ph)_6$, **4**

With the publication of the synthesis and structure of $Mo_2(CH_2Ph)_6$, Rothwell and coworkers demonstrated that stable M_2R_6 dimers could be formed with relatively small R groups [8]. Surprisingly, the dimolybdenum compound was not stabilized by η^3 interactions between the benzyl group and the metal, implying that perhaps other small groups, such as CH_2CF_3 or CH_2CHMe_2 , might give stable dimers. We have investigated this issue peripherally by synthesizing the hexa(benzyl)ditungsten compound **4**. In contrast to **3**, $W_2(OCMe_3)_6$ is an excellent starting material for this dimer. Complex **4** precipitates from the reaction mixture, simplifying its isolation considerably, although for best yield removal of solvent and trituration of the residue is necessary. The advantage of using the hexa(*t*-butoxide) dimer in place of the hexa(cyclohexoxide) dimer is that the $LiOCMe_3$ byproduct is easily removed by the trituration step. We have been unable to prepare **4** from $Na_2W_2Cl_7(THF)_5$.

We thought that the increased $W\equiv W$ bond length in **4** as compared to the $Mo\equiv Mo$ bond length in $Mo_2(CH_2Ph)_6$, and the consequent increased chance for decomposition by α - or γ -hydrogen abstraction by the metal, might mean that **4** would prove unisolable, but in fact the tungsten dimer is stable at room temperature when pure. It is, however, thermally sensitive; an NMR sample decomposed completely to uncharacterized materials within 1 hour at 50°C. Since the dimolybdenum compound is stable for several hours under similar conditions, it appears that the larger size of the ditungsten core in **4** does allow decomposition routes to become viable.

Rothwell et al., noted that the methylene resonance in the 1H NMR spectrum of $Mo_2(CH_2Ph)_6$, appeared at δ 3.70, a shift attributed to the deshielding caused by the diamagnetic anisotropy of the $Mo-Mo$ triple bond [8]. The analogous resonance in **4** appears at δ 3.64. The shift in

each case is ca. δ 1.6 from that of the parent hydrocarbon (toluene), similar to the shift observed for the methylene vs. Me_3SiPh in **2** and **3** (ca. δ 1.5; see Experimental). The observation holds for $\text{M}_2(\text{CH}_2\text{SiMe}_3)_6$ ($\text{M}=\text{Mo}$: δ 2.02; $\text{M}=\text{W}$: δ 1.90; $(\text{CH}_3)_4\text{Si}$: δ 0.00) and $\text{M}_2(\text{CH}_2\text{CMe}_3)_6$ ($\text{M}=\text{Mo}$: δ 2.75; $\text{M}=\text{W}$: δ 2.52; $(\text{CH}_3)_4\text{C}$: δ 0.90). Thus the additional data support Rothwell's hypothesis and suggest that the methylene resonance in an $\text{M}_2(\text{CH}_2\text{R})_6$ compound will generally lie 1.6–1.9 ppm downfield of the resonance in the organic parent.

Dimer **4** is isomorphous with the dimolybdenum compound. The $\text{W}\equiv\text{W}$ distance is 0.074 Å longer than the $\text{Mo}\equiv\text{Mo}$ distance, but this has only a minor impact on any of the other parameters. We noted above that the $\text{Mo}-\text{C}$ bond distance in $\text{Mo}_2(\text{CH}_2\text{Ph})_6$ appeared slightly longer than that in the other dimolybdenum compounds characterized. The same may hold for $\text{W}_2(\text{CH}_2\text{Ph})_6$: the $\text{W}-\text{C}$ distance of 2.156 (6) Å appears longer than that in **3**. However, the average $\text{W}-\text{C}$ distance in $\text{W}_2(\text{CH}_2\text{SiMe}_3)_6$ is 2.14 (4, 6, 12) Å, experimentally indistinguishable from the target value. This distance may be artifactually long, though, as the diffraction data for the hexa(trimethylsilylmethyl) compound were noted to be limited and of mediocre quality, so that the carbon atoms were refined isotropically [7]. More data are needed to address this point unambiguously.

The $\text{W}-\text{W}-\text{C}$ angle [98.36 (14)° vs. 97.61 (6)° for $\text{Mo}_2(\text{CH}_2\text{Ph})_6$] and $\text{W}-\text{C}-\text{C}$ angle [100.1 (3)° vs. 98.9 (1)° for $\text{Mo}_2(\text{CH}_2\text{Ph})_6$] open slightly, reflecting, as in the comparisons above, the need for the ligands to protect the larger dimetal core in **4** by occupying more space. The $\text{M}-\text{M}-\text{C}-\text{C}$ (phenyl) torsion angles are essentially identical for the molybdenum and tungsten homologues [143.4° and 143.7 (5)°, respectively], and are similar to that observed in **1**.

4. Conclusion

The goal of this work was to find general and optimal routes to dimolybdenum- and ditungsten hexaalkyls. While “ $\text{MoCl}_3(\text{dme})$ ” appears to be a general reagent for such syntheses, product yields are such that it cannot be termed an optimal one. Advantages of the trichloride include its easy preparation and the simple separation of the hexaalkyl product from byproducts, but its giving unpredictable yields cannot be overlooked when the required alkyllithiums are expensive to prepare. If one is interested in preparing a dimolybdenum hexaalkyl in the highest possible yield, Rothwell's route starting from $\text{Mo}_2(\text{O}-i\text{Pr})_6$ appears to be the best choice.

$\text{NaW}_2\text{Cl}_7(\text{THF})_5$ seems useful only for preparing the hexa(neopentyl)- or hexa-(trimethylsilylmethyl)ditungsten compounds. We had little success in preparing hexaalkyls using more reducing phenyl-substituted alkyllithiums, and we suspect this to be a general problem. We found

$\text{W}_2(\text{OCy})_6$ good for preparing some hexaalkyls, but forming this material requires several steps. Even when it is used, yields are not great. $\text{W}_2(\text{OCMe}_3)_6$, while useful for specific syntheses such as that of **4**, does not have broad applicability. Probably the bulky cyclohexoxy and *t*-butoxy groups slow the attack by the alkyllithium and allow side reactions to occur. Possibly $\text{W}_2(\text{O}-i\text{Pr})_6$, the homologue of Rothwell's dimolybdenum reagent, is the ideal starting point for the synthesis of ditungsten hexaalkyls, but it brings its own set of problems: it must be prepared and stored at low temperature to avoid dimerization [23] As a result, we have not tested its efficacy.

The structural data expand the database of homoleptic dimetal hexa(ligand) species and provide clear proof that the metal–metal triple-bond distance in dimetal hexaalkyls is inherently 0.06–0.08 Å shorter than that in dimetal hexaalkoxides. This has been known for a long time, but the matched pair of compounds reported here removes the possibility that the difference arises from steric concerns rather than electronic ones. The latter are clearly key, and we believe that the larger effective positive charge on the metals in the hexaalkoxides resulting from the greater electronegativity of oxygen vs. carbon causes the phenomenon.

It is interesting that the structural differences involving the alkyl ligands can be attributed to steric needs. One might have suspected that silyl-substituted alkyl ligands would display unique parameters arising from their relatively electron-rich character, but this does not appear so. Even more surprising is the fact that the hexa(benzyl) compounds are not remarkably different from the hexa-(primary alkyls), despite the electronic variations between benzyl and other primary alkyls. This suggests that computational chemists should be able to model most dimetal (hexaalkyls) as $\text{M}_2(\text{CH}_3)_6$ or $\text{M}_2(\text{CH}_2\text{CH}_3)_6$ species, simplifying the problem considerably.

Supplementary Material Available

Structural data have been deposited in the Cambridge Crystallographic Data Centre Structural Database [24]. Some data are also available from the primary authors upon request.

Acknowledgements

We appreciate the interest in and comments regarding this work of Professor Malcolm Chisholm, Indiana University, and Professor Richard Dallinger, Wabash College.

References

- [1] F. Huq, W. Mowat, A. Shortland, A.C. Skapski, G. Wilkinson, J. Chem. Soc., Chem. Commun. (1971) 1079.

- [2] M.H. Chisholm, Polyhedron 2 (1983) 681.
- [3] M.H. Chisholm, ChemTracts-Inorg. Chem. 4 (1992) 273.
- [4] F.A. Cotton, R.A. Walton, Multiple bonds between metal atoms. 2nd ed. Oxford: Clarendon, 1993.
- [5] W. Mowat, G. Wilkinson, J. Chem. Soc., Dalton Trans. (1973) 1120.
- [6] M.H. Chisholm, B.W. Eichhorn, K. Folting, et al., Inorg. Chem. 26 (1987) 3182.
- [7] M.H. Chisholm, F.A. Cotton, M. Extine, B.R. Stults, Inorg. Chem. 15 (1976) 2252.
- [8] S.M. Beshouri, I.P. Rothwell, K. Folting, J.C. Huffman, W.E. Streib, Polyhedron 5 (1986) 1191.
- [9] L. Chamberlain, J. Keddington, I.P. Rothwell, Organometallics 1 (1982) 1098.
- [10] T.M. Gilbert, A.M. Landes, R.D. Rogers, Inorg. Chem. 31 (1992) 3438.
- [11] J.C. Littrell, C.E. Talley, R.F. Dallinger, T.M. Gilbert, Inorg. Chem. 36 (1997) 760.
- [12] M.H. Chisholm, K. Folting, M. Hampden-Smith, C.A. Smith, Polyhedron 6 (1987) 1747.
- [13] M. Schlosser, J. Hartmann, Angew. Chem., Int. Ed. Eng. 12 (1973) 508.
- [14] R.R. Schrock, J.D. Fellman, J. Am. Chem. Soc. 100 (1978) 3359.
- [15] G. Sheldrick, SHELXTL. A suite of computer programs for X-ray structure determination, sold by Siemens Analytical Instruments, Inc., Madison, WI, USA.
- [16] M.N. Burnett, C.K. Johnson, ORTEP-III: Oak Ridge thermal ellipsoid plot program for crystal structure illustrations. Oak Ridge National Laboratory Report ORNL-6895, 1996.
- [17] Esds of averaged values are given as (a, b, c), where a is the average esd, b is the standard deviation of the individual values from the average, and c is the number of values averaged.
- [18] We note that diffraction data for $\text{Mo}_2(\text{CH}_2\text{Ph})_6$ were collected at 120 K, lower than the temperature used for any other dimer. Since bond distances normally decrease with lowered data collection temperature, this supports the argument that the M–C bond distance in the hexabenzyl compound is unusually long.
- [19] T.M. Gilbert, C.B. Bauer, A.H. Bond, R.D. Rogers, Polyhedron, preceding paper in this issue.
- [20] M.H. Chisholm, F.A. Cotton, B.A. Frenz, W.W. Reichert, L.W. Shive, B.R. Stults, J. Am. Chem. Soc. 98 (1976) 4469.
- [21] M.H. Chisholm, F.A. Cotton, C.A. Murillo, W.W. Reichert, Inorg. Chem. 16 (1977) 1801.
- [22] J.R. Pollard, T.M. Gilbert, D.L. Lichtenberger, J. Am. Chem. Soc., submitted.
- [23] M.H. Chisholm, D.L. Clark, K. Folting, J.C. Huffman, M. Hampden-Smith, J. Am. Chem. Soc. 109 (1987) 7750.
- [24] F.H. Allen, O. Kennard, R. Taylor, Acc. Chem. Res. 16 (1983) 146.